

See discussions, stats, and author profiles for this publication at: <https://www.researchgate.net/publication/265740776>

## CHAPTER 2 CLIMATE FORCING DURING THE HOLOCENE

Article · October 2003

DOI: 10.22498/pages.11.2-3.18

---

CITATIONS

24

READS

294

1 author:



Raymond S Bradley

University of Massachusetts Amherst

415 PUBLICATIONS 28,152 CITATIONS

SEE PROFILE

Some of the authors of this publication are also working on these related projects:



Canadian Arctic ice core paleo records [View project](#)



Nonstationary storm risk analyses over the past millennium [View project](#)

# CHAPTER

## 2

# CLIMATE FORCING DURING THE HOLOCENE

Raymond S. Bradley

**Abstract:** The role of several important factors that have played a role in Holocene climate change is examined. These forcing factors operate on different time-scales: lower frequency (millennial-scale) climate changes associated with orbital forcing, century-scale variability associated with solar forcing, and annual- to decadal-scale variability associated with volcanic forcing. Feedbacks within the climate system may involve non-linear responses to forcing, especially if critical thresholds are exceeded. In addition, there may be distinct regional climate anomaly patterns that result from certain types of forcing. Other anomalies that appear in Holocene paleoclimatic records may be unrelated to external forcing factors, but reflect conditions entirely within the climate system. General circulation model simulations play an important role in helping to understand how these various factors interact to produce the observed changes in Holocene climate.

**Keywords:** Orbital forcing, Solar forcing, Volcanic forcing

Why did climate change during the Holocene? The paleoclimatic records that are discussed at length in other chapters reflect, to a large extent, the composite effects of external factors operating on the climate system, plus feedbacks within the climate system that were triggered by these factors. Climate forcing (external factors that may cause climate to change) can be considered on several time-scales, ranging from very long-term (multi-millennial) to interannual. The resulting climate in any one region is the consequence of variability across all time-scales, but breaking the spectrum of climate variability down, from lower to higher frequencies, provides a useful way of assessing different forcing mechanisms. Here some of the main forcing factors during the Holocene are considered, beginning with factors operating at the lower frequency end of the spectrum.

## 2.1 ORBITAL FORCING

On the very longest, multi-millennial time-scales, the main factors affecting Holocene climate change are related to orbital forcing (changes in obliquity, precession and eccentricity). These changes involved virtually no change in overall global insolation receipts (over the course of each year) but significant re-distribution of energy, both seasonally and latitudinally. Representing the time- and space-varying nature of orbitally driven insolation anomalies is difficult in a single diagram, but Plate 1 shows these changes schematically for each month, with each panel representing the time-varying anomaly pattern over the last 10,000 years, with

respect to latitude. In the Early Holocene, precessional changes led to perihelion at the time of the northern hemisphere summer solstice (today it is closer to the winter solstice). This resulted in higher summer insolation in the Early Holocene at all latitudes of the northern hemisphere (ranging from  $\sim 40^\circ\text{W}/\text{m}^2$  higher than today at  $60^\circ\text{N}$  to  $25^\circ\text{W}/\text{m}^2$  higher at the Equator). Thus, July insolation (radiation at the top, or outside, the atmosphere) has slowly decreased over the last 12,000 years (See Plate 1). Anomalies during southern hemisphere summers were smaller, centred at lower latitudes, and they were opposite in sign (that is, insolation increased over the course of the Holocene). For example, January insolation anomalies were  $\sim 30^\circ\text{W}/\text{m}^2$  below current values at  $20^\circ\text{S}$  in the early Holocene.

What impact did such changes have on climate in different regions? Unfortunately, it is not a simple matter to translate insolation anomalies of solar radiation entering the atmosphere into radiation receipts at the surface, and it is even more difficult to then infer the effect of such changes on climate. Radiation passing through the atmosphere is reflected and absorbed differently from one region to another (depending to a large extent on the type and amount of cloud cover). Furthermore, surface albedo conditions also determine how much of the radiation reaching the surface will be absorbed. There may also be complexities induced in the local radiation balance. For example, Kutzbach and Guetter (1986) found that a 7 per cent increase in solar radiation at low latitudes, outside the atmosphere, at 9 ka BP was associated with 11 per cent higher net radiation at the surface due to a decrease in outgoing long-wave radiation (because of increased evaporation and higher water vapor levels in the atmosphere, which absorb long-wave radiation). However, this amplification of solar radiation effects was not as important at higher latitudes (where precipitation amounts are much less a function of solar radiation anomalies). Differences in surface properties may lead to changes in regional-scale circulation; for example, differential heating of land versus ocean (with the same insolation anomaly) could lead to land–sea circulation changes. Indeed, this effect served to drive an enhanced monsoon circulation over large parts of the northern continents in the Early Holocene, leading to wetter conditions and consequent changes in vegetation (see below). Finally, on an even larger scale, differential radiation anomalies from the Poles to the Equator may have led to changes in temperature gradients and consequent changes in the overall strength of atmospheric circulation, with associated shifts in the Hadley and extra-tropical circulation (Rind, 1998, 2000).

To assess such complexities under a constantly varying insolation regime requires general circulation model simulations. Numerous studies have examined the effects of orbital forcing for selected time intervals during the Holocene, initially using atmosphere global circulation models (GCMs; with fixed sea-surface temperatures: e.g. Kutzbach and Guetter, 1986; Hall and Valdes, 1997), then models with interactive ocean–atmosphere systems (e.g. Kutzbach and Liu, 1997; Hewitt and Mitchell, 1998) and, more recently, fully coupled ocean–atmosphere–biosphere models, where the interactions between the atmosphere and land surface hydrology and vegetation is treated explicitly (Brovkin *et al.*, 1996; Kutzbach, 1996; Coe and Bonin, 1997; Broström *et al.*, 1998). Most of these studies focus in particular on northern Africa where Early Holocene conditions were much wetter than the Late Holocene, and the transition between these states was quite abrupt, at around 5500 calendar years BP (deMenocal *et al.*, 2000a). All model simulations demonstrate that increased summer insolation in northern hemisphere summers, in the Early Holocene, caused a stronger monsoon circulation and increased precipitation in sub-Saharan Africa. However, unless vegetation and hydrological feedbacks are incorporated into the models, the precipitation amounts simulated

are well below those that would have been necessary to support the lakes and vegetation changes that are known (from the paleoclimatic record) to have occurred (Foley, 1994).

These conclusions have been obtained from model simulations, generally centred at specific time intervals (snapshots at 3000-year intervals) through the Holocene (e.g. Kutzbach, 1996; Joussaume *et al.*, 1999). With complex GCMs, given computational constraints, it is not feasible to run long, multi-millennia simulations to examine transient changes. However, the paleoclimatic record suggests that the gradual changes in insolation were not matched by equally gradual changes in surface climate over North Africa. Rather, the transition from arid to humid conditions was abrupt, both at the onset of wetter conditions (~14,800 calendar years BP and at its termination ~5500 calendar years BP). Both transitions correspond to summer (June–July–August (JJA)) insolation levels of ~4 per cent greater than today (outside the atmosphere) at 20°N. To investigate this, transient model simulations have been made for the last 9000 years, using a much lower resolution zonally-averaged model, (but with a coupled ocean–atmosphere system and vegetation feedbacks) (Claussen *et al.*, 1998, 1999; Ganopolski *et al.*, 1998a). These point to the importance of vegetation feedbacks as critically important; vegetation changes abruptly amplified the linear orbital influence on precipitation over North Africa, to produce an abrupt, non-linear change at ~5440 BP, corresponding to the paleoclimatic field evidence (Fig. 2.1). Although the North African case may be an extreme example of the role of vegetation feedbacks, other model simulations also suggest that vegetation changes at pronounced ecotones (such as the tundra–boreal forest interface) may also play a strong role in modifying initial forcing factors (Foley *et al.*, 1994; TEMPO, 1996; Texier *et al.*, 1997).

## 2.2 SOLAR FORCING

Orbital forcing involves the redistribution of incoming solar energy, both latitudinally and seasonally. Thus there are differential effects on the climate system that can lead to circulation changes, and there may be different responses to the forcing in the northern and southern hemispheres. Changes in solar irradiance (energy emitted by the sun) might be expected to affect all parts of the earth equally. However, this is not so because the response to solar irradiance forcing is amplified regionally, as a result of feedbacks and interactions within the atmosphere (Rind, 2002).

Until quite recently it was assumed (based on measurements in dry, high-altitude locations) that total irradiance did not vary, at least not on inter-annual to decadal scales – hence the term ‘solar constant’ was coined to describe the energy that is intercepted by the atmosphere when the sun is overhead ( $1368\text{ W/m}^2$ ) (National Research Council, 1994; Hoyt and Schatten, 1997). Satellite measurements over the last ~25 years tell a different story – total solar irradiance (TSI; that is, integrated over all wavelengths) varies by ~0.08 per cent over a Schwabe solar cycle (average length of ~11 years), with maximum values at times of maximum solar activity (when there are many sunspots and bright solar faculae; Lean, 1996; Fröhlich and Lean, 1998) (Fig. 2.2). Furthermore, irradiance changes at very short (ultraviolet) wavelengths vary even more over a solar cycle (Lean, 2000). Such changes have significance because an increase in UV radiation causes more ozone ( $\text{O}_3$ ) to be produced in the upper stratosphere; ozone absorbs radiation (at UV wavelengths of 200–340 nm) so heating rates in the upper atmosphere are increased during times of enhanced solar activity. This then affects stratospheric winds

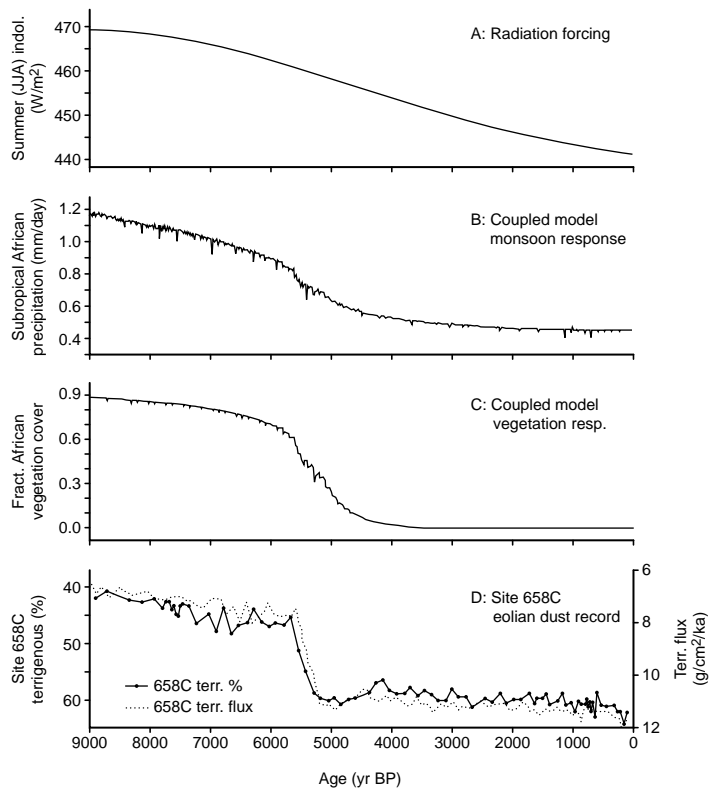


**Figure 2.1** Model simulations (Claussen *et al.*, 1999) of the response of North African precipitation (b) and fractional vegetation cover (c) compared to radiation forcing – summer (JJA) radiation at 20°N (a) and the record of eolian (Saharan) dust in a sediment core from off the west coast of North Africa (deMenocal *et al.*, 2000a). The model incorporates vegetation feedbacks that seem to be important in generating a non-linear response to orbital forcing, at ~5500 BP. Reprinted from deMenocal *et al.* (2000a), with kind permission from Elsevier Science.

(strengthening stratospheric easterlies), which can in turn influence surface climate via dynamical linkages between the stratosphere and the troposphere (Shindell *et al.*, 1999; Baldwin and Dunkerton, 2001; O’Hanlon, 2002). Model simulations of these effects indicate that there is a poleward shift of the tropospheric westerly jet and a poleward extension of the Hadley circulation, by ~70 km from solar minimum to solar maximum, in the summer hemisphere (Haigh, 1996; Larkin *et al.*, 2000). Although such changes are small, if irradiance changes in the past were larger and more persistent than solar cycle variability, the effects may have been quite significant.

How much has irradiance changed over longer time-scales? Satellite measurements are too short to shed light on longer-term irradiance changes, so these must be inferred from other lines of evidence. Lean *et al.* (1992) examined variations in brightness of stars similar to our own sun, concluding that present-day solar activity is at relatively high levels. By analogy with the range

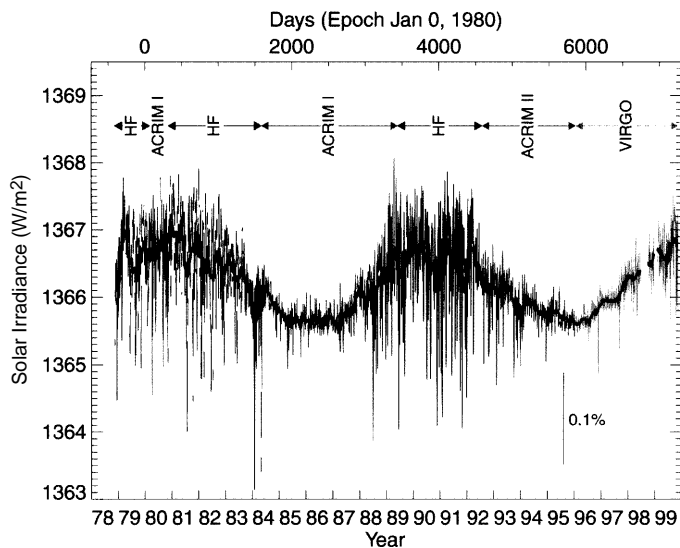


**Figure 2.2** Total solar irradiance as recorded by satellites since 1979 (Fröhlich, 2000). This energy is distributed only over the illuminated half of the earth which intercepts it over a circular area ('circle of illumination'). Considering the area of a sphere ( $4\pi r^2$ ) versus that of a circle ( $\pi r^2$ ), the average energy impinging at the top of the atmosphere is  $1368/4$ , or  $\sim 342^\circ\text{W m}^{-2}$  (Hoyt and Schatten, 1997). Hence a variation of 0.08% over an  $\sim 11$ -year (Schwabe) solar cycle is equivalent to a mean forcing of  $0.27^\circ\text{W m}^{-2}$ ; this is further reduced (by  $\sim 30\%$ ) due to planetary albedo effects (scattering, reflection) to  $\sim 0.2^\circ\text{W m}^{-2}$ . It should be born in mind, however, that the earth can not reach radiative equilibrium in relation to forcing over an 11-year solar cycle, as the ocean has great thermal inertia, which smoothes out the effects of rapid changes in external forcing. Reprinted from Fröhlich (2000) with kind permission from Kluwer Academic Publishers.

of brightness in stars like the sun, with or without activity cycles, they inferred that the historical range of TSI varied by  $\sim 0.24$  per cent, from the time of minimal solar variability at the end of the 17th century (the 'Maunder Minimum',  $\sim$ AD 1645–1715) to the present (i.e. the mean of the most recent solar cycle). Shorter-term ( $\sim 11$  years) variability of  $\sim 0.08$  per cent is superimposed on the lower frequency changes (Fig. 2.3). Simple comparisons with long-term temperature estimates suggest that changes in TSI of  $\sim 0.24$  per cent were associated with mean annual surface temperature changes over the northern hemisphere of  $0.2$ – $0.4$  °C (Lean *et al.*, 1995) and such changes have also been simulated in GCM and energy balance solar forcing experiments (Rind *et al.*, 1999; Crowley, 2000; Shindell *et al.*, 2001). Indeed, Crowley (2000) concluded that much of the low frequency variability in northern hemisphere temperatures over the last millennium (prior to the onset of global anthropogenic effects) could be explained in terms of solar and volcanic forcing. It is also interesting that distinct patterns of regional temperature change may be associated with solar forcing, as seen in both empirical and modelling studies, due to complex interactions between the circulation in the stratosphere and the troposphere (Shindell *et al.*, 2001; Waple *et al.*, 2001). Prolonged periods of reduced solar activity, like the Maunder Minimum, are associated with overall cooler conditions, but cooling is especially pronounced over mid- to high-latitude continental interiors, and warmer

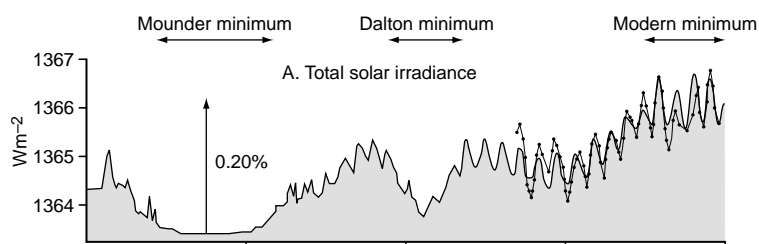


**Figure 2.3** Estimated variability in total solar irradiance (TSI) over the last 400 years (Lean, 2000); cf. Fig. 2.3 for the most recent Schwabe solar cycles.

temperatures occur over mid- to high latitudes of the Atlantic. Such a pattern is characteristic of a shift in the North Atlantic Oscillation (NAO) towards lower index conditions, whereby the pressure gradient between Iceland and the Azores is reduced, leading to less advection of warm, moist air from the Atlantic into western Europe, and cooler temperatures over Eurasia. Shindell *et al.* (2001) simulated winter temperatures over eastern North America and western Europe that were cooler by 1–2 °C during the late Maunder Minimum, compared to a century later when solar irradiance was higher (Plate 2). Such changes are consistent with the paleoclimatic evidence (Pfister *et al.*, 1999; Luterbacher *et al.*, 2001).

If solar irradiance has changed by ~0.24 per cent over the last 350 years, how much change occurred during the Holocene? Long-term changes in solar activity can be estimated from changes in cosmogenic isotopes preserved in natural archives. Cosmic rays intercepted by the upper atmosphere produce cosmogenic isotopes – such as  $^{10}\text{Be}$  and  $^{14}\text{C}$  – which eventually enter the terrestrial environment at the earth's surface. During times of high solar activity the flux of cosmic rays to the atmosphere is reduced, leading to a reduction in the production rate of these isotopes. Thus, variations in cosmogenic isotopes are inversely related to solar activity. If we make the assumption that solar activity is correlated with TSI changes (as observed in the recent instrumental period – see Beer *et al.*, 1996), long-term changes in  $^{14}\text{C}$  (seen as departures from expected age, in tree-rings) or  $^{10}\text{Be}$  (in ice-cores) can be used as an index of solar irradiance changes over time. Unfortunately, other factors have also affected the production rate of cosmogenic isotopes over the Holocene, and these must be accounted for in order to isolate the effects of solar variability. In particular, magnetic field variations have had a large impact on production rates (a weaker field being associated with higher production levels). Also, changes in the rate at which radiocarbon was sequestered in the deep ocean (due, for example, to thermohaline circulation changes) may also have affected atmospheric concentrations in radiocarbon over the Holocene. To examine this question for the last millennia, Bard *et al.* (2000) used a box model of ocean carbon variations driven by  $^{10}\text{Be}$  variations measured in an ice-core to assess whether  $^{14}\text{C}$  variations over the last 1000 years had been affected by ocean circulation changes. On this time-scale, such effects appear to have been minimal, suggesting that  $^{14}\text{C}$  can be used to assess solar variability over the last thousand years and perhaps longer. A similar result was found by Beer *et al.* (1996) for the last 4000 years. In the last millennium, both  $^{10}\text{Be}$  and  $^{14}\text{C}$  indicate that solar activity was high from ~AD 1100 to 1250, decreased to minima in the 15th century and at the end of the 17th century, then increased in the 20th century to levels that were similar to those of the 12th century (Fig. 2.4). Detailed  $^{10}\text{Be}$  records are not yet available for the Holocene, but deviations of  $^{14}\text{C}$  from background levels (adjusted for magnetic field changes) reveal a large number of solar activity anomalies comparable to the

Maunder Minimum (as well as episodes of enhanced solar activity) throughout the Holocene (Stuiver and Braziunas, 1993b) (Fig. 2.5). Using the Maunder Minimum as a guide, the variability of  $\Delta^{14}\text{C}$  suggests that TSI may have varied by  $\pm 0.4$  per cent from modern levels during the Holocene.

If climatic conditions during the Maunder Minimum were driven by solar forcing alone, there ought to have been many similar climatic episodes during earlier periods. In fact, there are many Holocene paleoclimatic studies that claim solar forcing has driven observed changes,

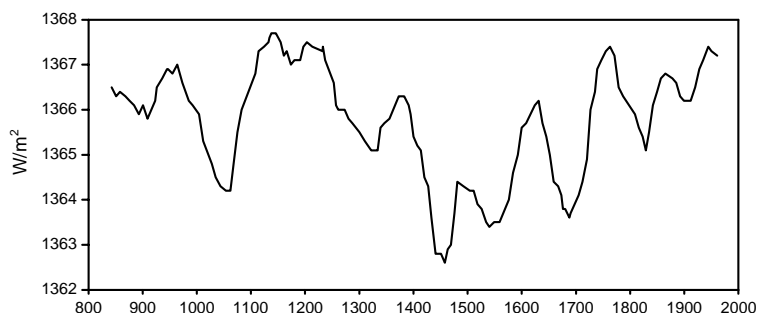


**Figure 2.4** Total solar irradiance from AD 843 to 1961, estimated from  $^{10}\text{Be}$  variations, recorded in an Antarctic ice-core, scaled to the estimates of Lean *et al.* (1995) (cf. Fig. 2.4). Other estimates of the magnitude of change in TSI from the Maunder Minimum to the present are higher – up to 0.65%, which, if correct, would simply amplify the scale of change shown here (data from Bard *et al.*, 2000).

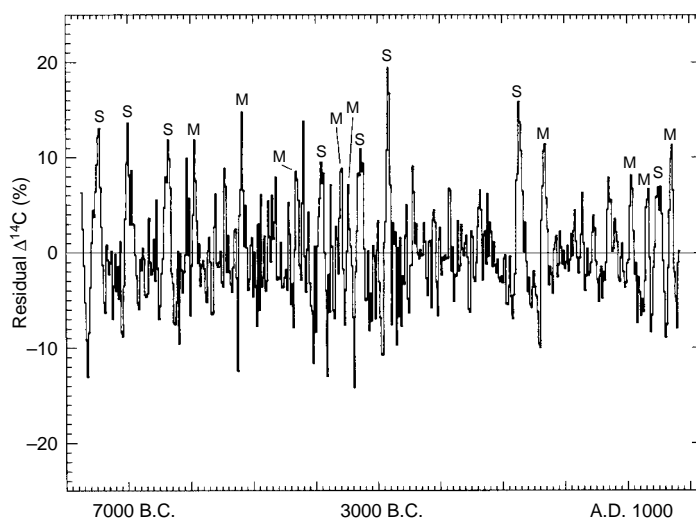


**Figure 2.5** Solar activity variations (lower values indicating higher solar activity/enhanced irradiance), as recorded by radiocarbon variations in tree-rings of known calendar age (after taking geomagnetic field effects into account) M = Maunder Minimum-like events; S = Sporer Minimum-like events. Reprinted from Stuiver *et al.* (1991), with kind permission from Elsevier Science.



based largely on comparisons of proxy records with the  $^{14}\text{C}$  anomaly series. In particular, paleoclimatic records of precipitation variability across the tropics, from northern South America and Yucatan (Black *et al.*, 1999; Haug *et al.*, 2001; Hodell *et al.*, 2001) to East Africa and the Arabian Peninsula (Verschuren *et al.*, 2000; Neff *et al.*, 2001), show strong correlations with solar activity variations recorded by  $^{14}\text{C}$  anomalies (e.g. Fig. 2.6). Furthermore, solar variability may also have played a role in mid-continental drought frequency on both short and long time-scales (Cook *et al.*, 1999; Yu and Ito, 1999; Dean *et al.*, 2002). Other studies have also identified potential links between solar activity variations and climate changes in the Holocene (Magny, 1993b; van Geel *et al.*, 2000). Bond *et al.* (2001) argue that temporal variations in the abundance of ice-rafted debris in North Atlantic sediments vary with the same frequency ( $\sim 1450\text{--}1500$  years) as  $^{14}\text{C}$  anomalies, and Stuiver *et al.* (1991) also noted the similarity between a  $\sim 1470\text{-year}$  periodicity in  $^{14}\text{C}$  data and a similar periodicity in oxygen isotopic data from GISP2. It remains to be seen how robust these relationships are, and what plausible mechanism might link solar activity/irradiance variations with climate in such diverse parts of the globe, from the Arabian Sea to the mid-continental USA, to Greenland. One possibility (seen in some model simulations) involves solar variations influencing the Hadley circulation (intensity and/or extent), which then leads to tropical and sub-tropical precipitation anomalies, and further teleconnections to extra-tropical regions.

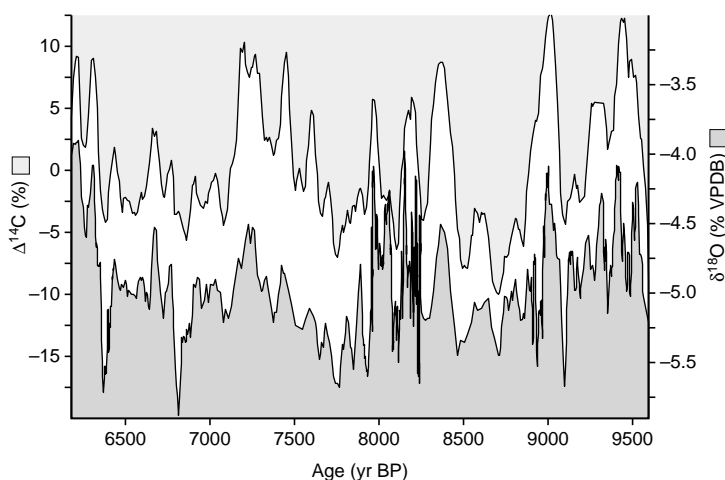


**Figure 2.6** The relationship between  $\delta^{18}\text{O}$  in an Early Holocene speleothem from Oman (representing rainfall, with lower values indicating wetter conditions) and  $\Delta^{14}\text{C}$ , representing solar activity variations (lower values indicating higher solar activity/enhanced irradiance). Reprinted from Neff *et al.* (2001), with kind permission from Macmillan Publishers Ltd.

## 2.3 VOLCANIC FORCING

It is well known, from studies of instrumental records, that explosive volcanic eruptions can have short-term cooling effects on overall hemispheric or global mean temperatures (Bradley, 1988; Robock, 2000). These result from direct radiative effects, with the volcanic aerosol reducing energy receipts at the surface, plus associated circulation changes that may result from

such effects. Such circulation changes (often involving an amplification of the upper Rossby wave pattern) lead to large negative temperature anomalies in some regions, but other areas may become warmer. For example, it has been noted that warming in high-latitude continental interiors, in winter months, was commonly associated with major eruptions during the 20th century (Groisman, 1992; Robock and Mao, 1992, 1995).

Most temperature effects are not detectable after a few years, so individual explosive eruptions only contribute short-term variability to the spectrum of Holocene climate. However, if eruptions were more frequent in the past, or if they happened to occur in clusters of events, it is possible that the cumulative effect of eruptions could have persisted for longer, resulting in decadal- to multi-decadal-scale impacts. Such effects would be enhanced if the initial cooling led to feedbacks within the climate system, such as more persistent snow and sea-ice cover, which would raise the surface albedo and possibly alter the atmospheric circulation. Sulphate levels in ice-cores from Greenland provide an index of explosive volcanism in the past, albeit possibly biased towards high-latitude eruption events (Fig. 2.7). The GISP2 record suggests that there were indeed periods of more frequent events in the past, such as in the period 9500–11,500 calendar years BP (Zielinski *et al.*, 1994). Furthermore, in the early Holocene, there were many more large volcanic signals greater than that recorded after the eruption of Tambora (1815) which was the largest eruption in recent centuries (registering 110 ppb of volcanic sulfate at the GISP2 site in central Greenland) (Fig. 2.7). Of course, a larger sulphate signal might simply mean the eruption event was closer to the deposition site so we do not have a definitive long-term record of the magnitude of overall volcanic forcing, or more specifically, the record of atmospheric optical depth and its distribution latitudinally (cf. Roberston *et al.*, 2001). Nevertheless, energy balance and GCM studies that have attempted to parameterize the effects of explosive volcanism over recent centuries (where several lines of evidence can be combined to resolve the location and magnitude of each event) suggest that explosive volcanism has contributed to the natural variability of hemispheric and global mean temperatures over this interval of time (Crowley and Kim, 1999; Free and Robock, 1999; Crowley, 2000; Ammann *et al.*, 2002). Explosive volcanism, together with solar forcing, explains most of the variability of temperatures over the last millennium, so it seems likely that these two factors have also played a significant role in overall Holocene forcing, with volcanism having been of particular importance at certain times. Recent studies, for example, suggest that unusually cold conditions

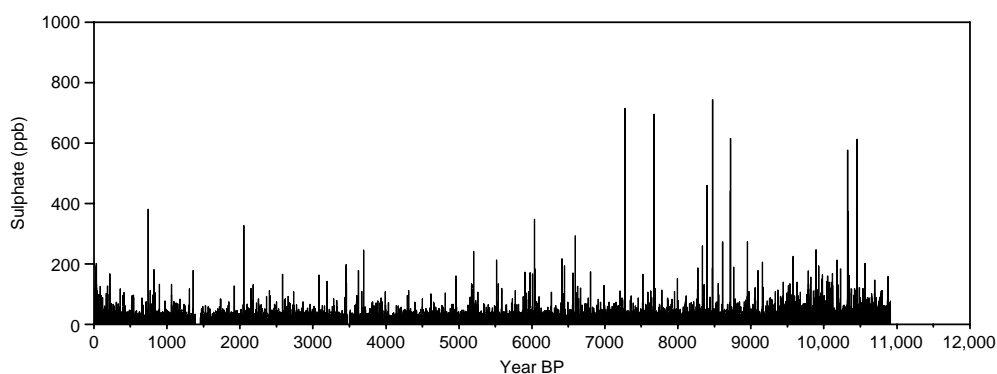


**Figure 2.7** The Holocene record of volcanic sulfate (anomalies from background variations) recorded in the GISP2 ice-core from Summit, Greenland (Zielinski *et al.*, 1994).

occurred in western Europe and southern Alaska in the latter half of the solar Maunder Minimum, because this period also coincided with an episode of exceptionally active explosive volcanism (Bauer *et al.*, 2002; Cubasch, 2002; D'Arrigo *et al.*, 2002, Shindell *et al.*, 2002).

## 2.4 DISCUSSION

Most paleoclimatic studies that cite a relationship to particular forcing mechanisms do so either via simple correlations in the time domain (curve-matching) or in the frequency domain (finding a spectral peak that corresponds to something similar in a particular forcing factor; e.g. Black *et al.*, 1999; Bond *et al.*, 2001). There has generally been little interaction between those working at the frontiers of understanding how forcings affect the climate system, in a mechanistic or dynamic sense, and those observing the paleoclimatic record (though see Friis-Christensen *et al.*, 2000). Modelling provides a link between these two approaches, particularly when simulations involve coupled ocean–atmosphere GCMs (with a realistic stratosphere), incorporating vegetation and land–surface (hydrological) feedbacks. With such tools, it may be possible to comprehend the complex interactions that are driven by what often appears to be a simple forcing function (most commonly exemplified by a simple plot of insolation anomalies for a particular latitude and month!). With such models, the spatial climatic response to particular forcing factors can be determined, and perhaps thresholds and feedbacks within the system can also be identified (as suggested by Fig. 2.1) to help explain the observed Holocene paleoclimatic record.

Finally, it must be recognized that not all paleoclimatic variability seen in the Holocene can (or should) be ascribed to specific external forcings. Perhaps the best example of this is the ~8200 calendar year BP ‘event’, seen in many paleoclimatic archives, that resulted from catastrophic pro-glacial lake drainage at the margins of the Laurentide Ice Sheet (Alley *et al.*, 1997; Barber *et al.*, 1999; Baldini *et al.*, 2002). This rapid flooding of the North Atlantic with freshwater clearly had a significant regional impact, unrelated to any external forcing. There are also internal modes of climate system variability (e.g. El Niño Southern Oscillation, North Atlantic Oscillation, Pacific Decadal Oscillation) that likely vary on both long and short time-scales (though we know relatively little about their long-term behaviour). Furthermore, stochastic resonance in the climate system – by which a weak quasi-periodic forcing signal may be amplified into a non-linear, bi-stable climate signal – may have brought about relatively abrupt changes in the past by pushing the system across critical thresholds (Lawrence and Ruzmaikin, 1998; Ruzmaikin, 1999; Rahmstorf and Alley, 2002).

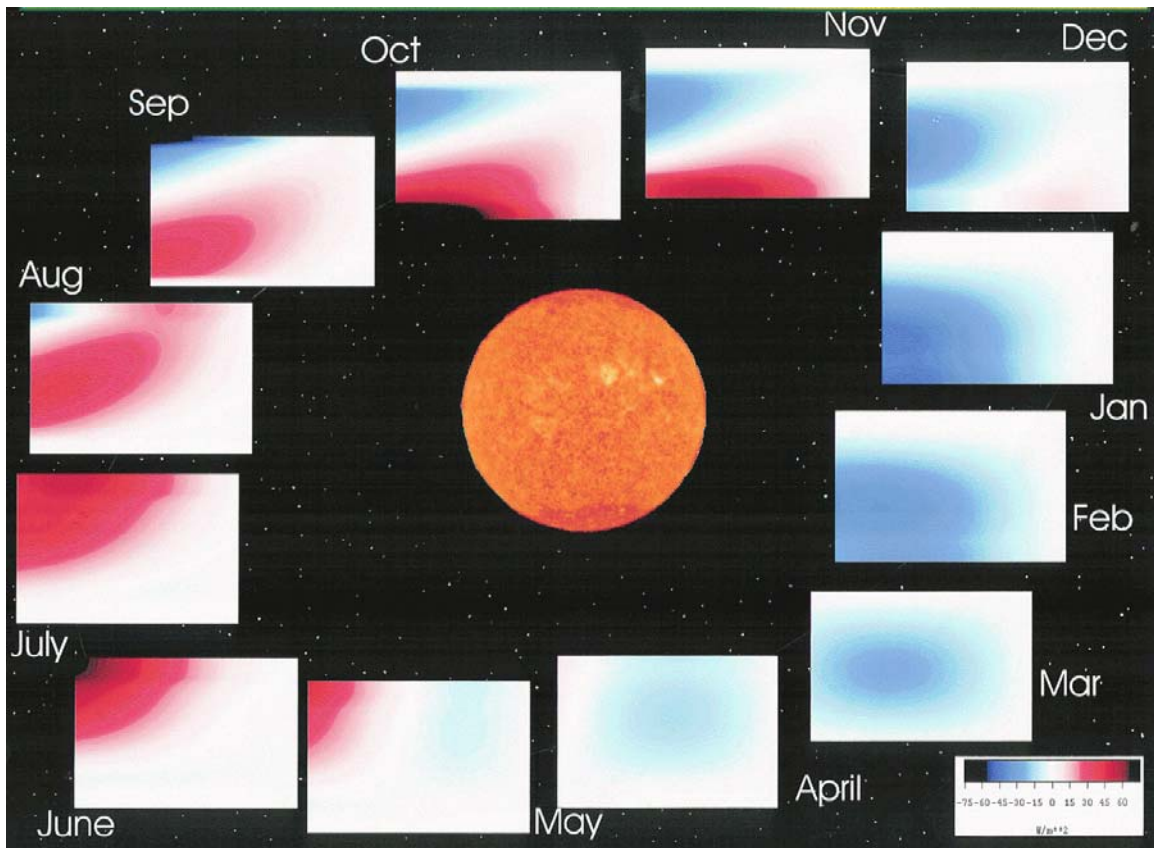


**Plate 1. Schematic representation of insolation anomalies at the top of the atmosphere, relative to 1950 levels. Anomalies are colour-coded in  $Wm^{-2}$ . Each *monthly panel* shows (on the x-axis): changes from 10,000 calendar years B.P. (left) to today (right), and on the y-axis: latitude, from 90°N at the top, to 90°S at the bottom (figure prepared by A. Waple).**

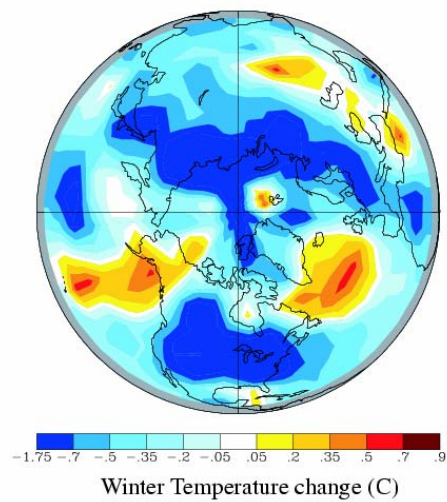
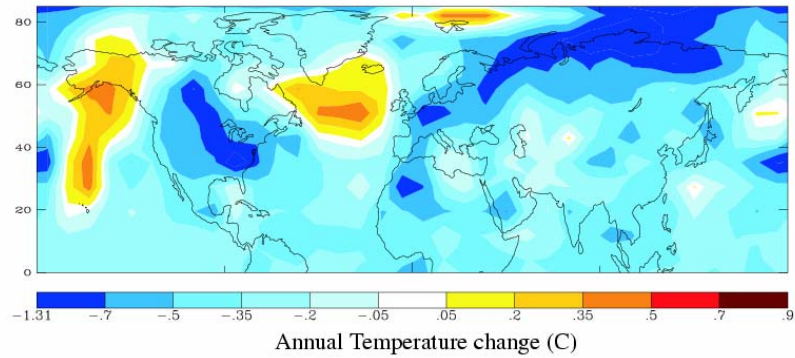


**Plate 2. Modelled winter (November to April) temperature difference between A.D. 1780 and 1680, showing the temperature “anomalies” associated with the late Maunder Minimum of solar activity, relative to a period (1780) with higher levels of activity (cf. Figure 4) (Shindell et al., 2001). Nearly all points are statistically significant (not shown) because of the large number of model years.**